

## The association of immune cell infiltration and prognostic value of tertiary lymphoid structures in gastric cancer

Ji-Shang YU<sup>1,2,\*</sup>, Wei-Bin HUANG<sup>1,\*</sup>, Yu-Hui ZHANG<sup>1,\*</sup>, Jian CHEN<sup>1,2</sup>, Jin LI<sup>2,3</sup>, Hua-Feng FU<sup>1,2</sup>, Zhe-Wei WEI<sup>1,\*</sup>, Yu-Long HE<sup>1,3,\*</sup>

<sup>1</sup>Department of Gastrointestinal Surgery, The First Affiliated Hospital, Sun Yat-sen University, Guangzhou, Guangdong, China; <sup>2</sup>Laboratory of General Surgery, the First Affiliated Hospital, Sun Yat-sen University, Guangzhou, Guangdong, China; <sup>3</sup>Center of Digestive Diseases, The Seventh Affiliated Hospital, Sun Yat-sen University, Shenzhen, Guangdong, China

\*Correspondence: heyulong@mail.sysu.edu.cn; denisewei@126.com

\*Contributed equally to this work.

Received January 28, 2022 / Accepted May 4, 2022

Tertiary lymphoid structures (TLS) are lymphoid aggregates in tumor tissues and their potential significance in clinical applications has not been fully elucidated in gastric cancer. We evaluated TLS and tumor-infiltrating immune cells using H&E and immunohistochemistry staining in the recruited patients with gastric cancer. The prognostic value of TLS was evaluated by Kaplan-Meier analysis and further validated using gene expression profiling. The alterations in gene mutation, copy number variance, and DNA methylation across the TLS signature subtypes were analyzed based on the Cancer Genome Atlas cohort. High TLS density was associated with improved overall survival and disease-free survival. A combination of TLS density and TNM stage obtained higher prognostic accuracy than the TNM stage alone. Tumors with high TLS density showed significantly higher infiltration of CD3<sup>+</sup>, CD8<sup>+</sup>, and CD20<sup>+</sup> cells but lower infiltration of CD68<sup>+</sup> cells. Transcriptomics analysis demonstrated that high TLS signature status was positively associated with the activation of inflammation-related and immune-related pathways. Multi-omics data showed a distinct landscape of somatic mutations, copy number variants, and DNA methylation across TLS signature subtypes. Our results indicated that TLS might link with enhanced immune responses, and represent an independent and beneficial predictor of resected gastric cancer. Multi-omics analysis further revealed key tumor-associated molecular alterations across TLS signature subtypes, which might help explore the potential mechanism of the interaction between TLS formation and cancer cells.

*Key words: tertiary lymphoid structures; immune infiltration; gastric cancer; prognosis*

Gastric cancer was ranked as the fifth most common human cancer, causing the fourth highest cancer-related mortality worldwide [1]. Radical gastrectomy is routinely the most effective treatment for localized tumors [2]. Even after potentially curative resection, the prognosis of gastric cancer patients remains poor because of the diagnosis at an advanced stage and frequent recurrence [3]. Therefore, early diagnosis, accurate prognostic assessment, and innovative therapeutic approaches are of utmost importance. At present, immune checkpoint inhibitors, which have proven highly effective in reactivating antitumor immune responses, have revolutionized cancer treatment in various solid malignancies [4, 5]. However, the response rate of gastric cancer patients to immunotherapy remains relatively low [6, 7]. The tumor microenvironment reflects the interaction between the immunological response and tumor development, which is a key factor affecting antitumor immunotherapy. To predict

the outcome and immunotherapy efficacy for gastric cancer, more extensive characterization of the tumor microenvironment is required.

Recent studies on the tumor microenvironment revealed that tertiary lymphoid structures (TLS), which are aggregates of immune cells at the tumor site, directly play a vital role in the modulation of antitumor defense [8]. TLS highly resemble secondary lymphoid organs in terms of structure and function. Structurally, TLS are immune cell aggregates with B cell lymphoid follicles surrounded by T cells. They are present in tumor tissues in two forms: early TLS and mature TLS [9]. Early TLS are vague or round clusters of lymphocytes without germinal center reactions. Mature TLS are well-formed lymphocyte clusters with germinal center formation, including activated dendritic cells (DCs) and high endothelial venules [10]. Functionally, tumor-associated TLS formation is a tumor antigens-driven process sustained by

tumor-associated inflammation [11, 12]. Located in the tumor core or invasive margin, TLS represent pivotal sites of adaptive immunity through activation and maintenance of T and B cell responses, resulting in the generation of effector cytokines and cytotoxic molecules by T cells and antitumor antibodies by B cells [8, 13]. Despite the known role of TLS in tumor progression, their formation and function in solid tumors have not been thoroughly explained so far. Accumulating evidence has shown that high densities of TLS were associated with favorable clinical outcomes in colorectal cancer [9], hepatocellular carcinoma [14], lung cancer [15], breast cancer [16], and melanoma [17], indicating that TLS could be a predictive and prognostic factor in solid tumors. In gastric cancer, He et al. [18] reported that a high level of TLS in gastric cancer patients was a positive indicator of overall survival (OS) based on hematoxylin and eosin staining (H&E) staining. However, TLS evaluation was less accurate by H&E staining alone, and the lack of uniform criteria to assess their distribution, density, and maturity limits translation into clinical practice [8, 18]. Furthermore, the correlation between TLS and tumor-infiltrating immune cells remains largely unexplored. In this study, we aimed to investigate the clinical significance of TLS and their association with tumor-infiltrating immune cells and molecular alterations in gastric cancer.

## Patients and methods

**Patients and data collection.** We retrospectively reviewed the data of patients with gastric cancer in the database of the First Affiliated Hospital of Sun Yat-sen University between 2009 and 2014. The inclusion criteria were as follows: 1) pathologically proven primary gastric adenocarcinoma; 2) no distant metastasis; 3) adequate tissue slides with tumor components and invasive margins; 4) lack of preoperative cancer treatment; and 5) complete clinicopathological records and follow-up information. Finally, eligible formalin-fixed paraffin-embedded specimens from 118 patients who underwent curative-intent resection were obtained and used in this study. For each patient, the tumor pathological stage was diagnosed according to the 8<sup>th</sup> edition of the Union for International Cancer Control. The follow-up period was dated to May 2019. OS was defined as the time from curative gastrectomy to the date of either death or the last follow-up. Disease-free survival (DFS) was defined as the time from surgical resection to the date of recurrence or the last follow-up. The current study was conducted in accordance with the Declaration of Helsinki and was approved by the Ethics Committee of the First Affiliated Hospital of Sun Yat-sen University.

**Immunohistochemistry.** Immunohistochemical staining was performed following standard procedures. Briefly, paraffin-embedded tumor samples were cut into 4  $\mu$ m thick serial sections. Tissue sections were heated at 60°C for 2 h, deparaffinized in xylene, and rehydrated using graded

alcohol. Sections were then subjected to antigen retrieval by high-pressure cooking in 10 mM citrate buffer (pH 6.0). Before antibody incubation, the specimens were quenched for endogenous peroxidase activity in 3% H<sub>2</sub>O<sub>2</sub> for 15 min and incubated in 3% bovine serum albumin for 30 min. Sections were incubated at 4°C overnight with primary antibodies: rabbit anti-CD20 (Abcam, ab78237, 1:200); rabbit anti-CD3 (Abcam, ab16669, 1:100); mouse anti-CD8 (Dako, M7103, 1:100); rabbit anti-CD11c (Abcam, ab52632, 1:500); rabbit anti-CD68 (Abcam, ab213363, 1:8000). Subsequently, sections were immunostained using Envision+System-HRP (Dako, K4005) and counterstained with hematoxylin.

**Method for TLS and immune cell quantification.** Slides were digitally scanned using a Zeiss Axio scan.z1 (Jena, Germany), operated with ZEN software. TLS were identified as lymphoid aggregates and quantified using both H&E and CD20 immunohistochemistry staining slides. TLS were evaluated in the whole slide including the intratumoral area and peritumoral area. The intratumoral area was defined as the tumor tissue area inside the infiltrative tumor front. The peritumoral area was defined as the adjacent non-tumoral tissue within a 5 mm region from the infiltrative tumor front. Because TLS were aggregates of lymphocytes, TLS density was analyzed by a normalization of the area [19, 20]. Intratumoral TLS density was measured as a percentage of the tumor area: [intratumoral TLS area (mm<sup>2</sup>)/tumor area (mm<sup>2</sup>)] $\times$ 100. Peritumoral TLS density was measured as a percentage of the adjacent non-tumoral area: [peritumoral TLS area (mm<sup>2</sup>)/peritumoral area (mm<sup>2</sup>)] $\times$ 100. The sum TLS density was calculated by adding intratumoral TLS density and peritumoral TLS density. The sum TLS density was used for subsequent data analysis because it completely reflected the TLS distribution in gastric cancer tissues. We also evaluated the presence of a germinal center in the TLS using H&E slides [21].

Quantitative analysis of immune cells was conducted separately at the tumor margin (TM) and tumor center (TC). Five representative fields (200 $\times$  magnification) per area were selected for the evaluation of positive immune markers. The number of stained cells was counted with ImageJ and converted to cell density (positive cell number/mm<sup>2</sup>). The evaluation of TLS and immune cell density was performed independently by two pathologists (Lu XF and Ding L). If the results of the evaluation were obviously heterogeneous, the two pathologists worked cooperatively to provide the final result.

**Bioinformatics analysis.** Microarray data and the corresponding clinical characteristics of gastric cancer tissues were obtained from the Gene Expression Omnibus (GEO) database, including GSE26899, GSE13861, GSE26901, GSE26253, GSE62254, and GSE28541 datasets, etc. [22]. The clinical and molecular features of The Cancer Genome Atlas Stomach Adenocarcinoma (TCGA-STAD) cohort were obtained from another study [23]. The TLS signature of gastric cancer was used in our study, and the

'ssGSEA' method was applied in the estimation of gene-set enrichment scores per sample via the R package 'GSVA' (v1.36.3) [8, 24]. Patients were divided into two TLS signature subtypes (high/low) according to the median value of 'ssGSEA' scores. Immune cell deconvolution from bulk tumor samples using the xCell method was completed via R package 'immunedeconv' (v2.0.3). Gene set enrichment analysis (GSEA) was performed using the R package 'clusterProfiler' (v3.16.1). Genomic data of the TCGA-STAD cohort, including RNA expression matrixes, gene mutation information, and DNA methylation profiles, were accessed through the R package 'TCGAbiolinks' (v2.16.4). Methods for the identification of epigenetically silenced genes across samples have been described previously [23]. Differentially epigenetically silenced genes across the TLS signature subgroups were identified via Fisher's exact test. To identify more representative silenced genes and CpG island probes across the TLS signature subtypes, we retained the following genes: a) with adjusted p-value <0.05 (Benjamini-Hochberg method) in differential analysis; b) methylated in over 25% samples in TLS-high/low subtype; c) not filtered in 'Boruta' (v7.0.0) feature selection based on RNA expression (log2 FPKM). We retained CpG island probes that were: a) differentially expressed across TLS subtypes according to the 'ChAMP' pipeline; b) part of appearing in the result of differentially epigenetically silenced gene analysis above.

**Statistical analysis.** SPSS software (v25.0), GraphPad Prism software (v9.0), R (v4.0.3), and MedCalc software (v20.0) were used for statistical analysis. The optimal cut-off for TLS density was selected on basis of the patients' 3-year DFS using the MedCalc software. For categorical variables, the correlations between TLS density and the clinicopathological features were analyzed using the chi-square test or Fisher's exact test. For continuous variables, the differences between groups were compared using Student's t-test or Mann-Whitney U-test. Survival outcomes were estimated using the Kaplan-Meier method and compared using log-rank tests. Univariate analysis was conducted to investigate the correlation between clinicopathological features and survival outcomes. Significant variables in the univariate analysis were subjected to multivariate analysis based on the Cox proportional hazards method (backward method). All statistical analyses were two-sided, and the statistical significance was set at  $p < 0.05$ .

## Results

**Characteristics and distribution of TLS in gastric cancer.** We assessed the distribution and cellular composition of TLS in serial sections of 118 patients with gastric cancer from the First Affiliated Hospital of Sun Yat-sen University (Figure 1A). Histologically, TLS were oval or irregular aggregates, similar to the organization of a lymph node, but did not contain membranes. Most CD20<sup>+</sup> B cells were located in the center of the follicle, while CD3<sup>+</sup> and CD8<sup>+</sup> T cells were

mainly distributed in the parafollicular zone. CD11c<sup>+</sup> DCs were discretely distributed within the TLS and CD68<sup>+</sup> tumor-associated macrophages (TAMs) were seldomly observed (Figure 1B).

**Clinicopathological characteristics and prognostic value of TLS.** To separate patients with low and high TLS densities, the cut-off value was obtained at 2.40 for TLS density on the basis of the receiver operating characteristic (ROC) (Figures 2A, 2B). Correlations between TLS and clinical features were further analyzed and were summarized in Table 1. TLS-high was positively correlated with lower pT category ( $p=0.043$ ), lower tumor-node-metastasis (TNM) stage ( $p=0.042$ ), and smaller tumor size ( $p=0.008$ ), indicating

**Table 1.** Association between TLS and clinical characteristics in gastric cancer.

Characteristics	N	TLS		
		low	high	p-value
All cases	118	65	53	
Gender				0.548
male	82	47	35	
female	36	18	18	
Age				0.136
<60 years	66	32	34	
≥60 years	52	33	19	
pT category				<b>0.043</b>
T1-2	35	14	21	
T3-4	83	51	32	
pN category				0.059
N0	48	21	27	
N1-3	70	44	26	
pStage				<b>0.042</b>
I	28	11	17	
II	38	19	19	
III	52	35	17	
Tumor size				<b>0.008</b>
<4 cm	73	33	40	
≥4 cm	45	32	13	
CEA				0.091
normal	89	45	44	
elevated	29	20	9	
CA199				0.146
normal	97	50	47	
elevated	21	15	6	
Location				0.851
antrum	46	26	20	
no antrum	72	39	33	
Histological type				0.457
undifferentiated	66	34	32	
differentiated	52	31	21	
Chemotherapy				0.355
yes	62	37	25	
no	56	28	28	

Abbreviations: TLS-tertiary lymphoid structures; CEA-carcinoembryonic antigen; CA199-Carbohydrate antigen199

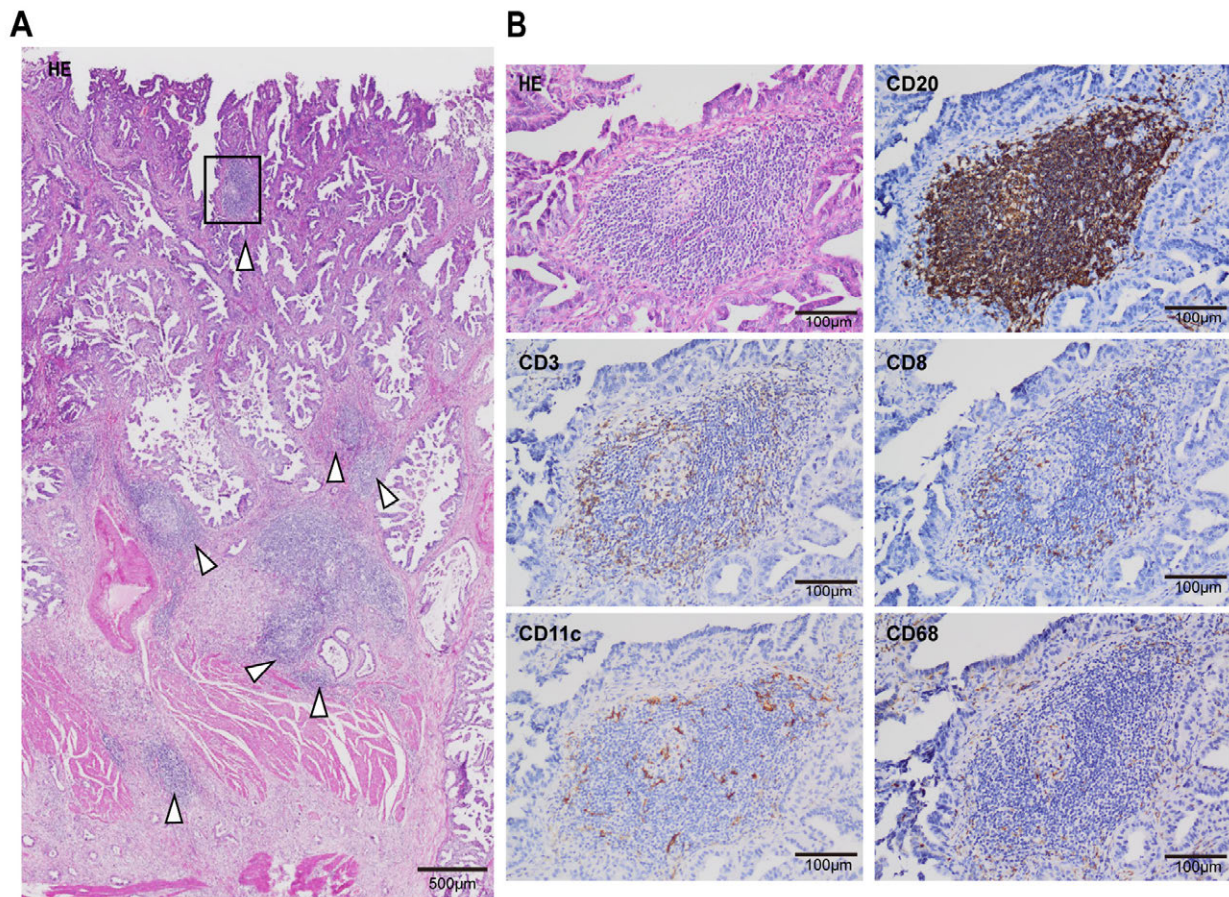


**Figure 1.** Representative images showing histological appearance and cellular composition of TLS in gastric cancer. A) H&E staining showing the appearance and distribution of TLS in gastric cancer tissue (white arrowheads). B) H&E and immunohistochemical analyses showing TLS components, including CD3<sup>+</sup> T cells, CD8<sup>+</sup> T cells, CD20<sup>+</sup> B cells, CD11c<sup>+</sup> DCs, and CD68<sup>+</sup> TAMs. TLS-tertiary lymphoid structures; H&E-hematoxylin and eosin; DCs-dendritic cells; TAMs-tumor-associated macrophages.

**Table 2.** Multivariate analyses of OS and DFS with TLS and clinical characteristics in gastric cancer.

Multivariable analysis Variable	Overall survival		Disease-free survival	
	Hazard ratio (95% CI)	p-value	Hazard ratio (95% CI)	p-value
CEA (elevated/normal)	1.358 (0.776–2.379)	0.284	1.357 (0.788–2.337)	0.271
CA199 (elevated/normal)	1.944 (1.040–3.634)	0.037	1.795 (0.964–3.343)	0.065
Chemotherapy (yes/no)	1.294 (0.737–2.272)	0.369	1.142 (0.655–1.992)	0.64
tumor size (≥ 4 cm/< 4 cm)	1.328 (0.758–2.327)	0.322	1.348 (0.779–2.334)	0.286
Stage (III/I+II)	5.923 (3.152–11.129)	<0.001	5.124 (2.828–9.282)	<0.001
TLS (high/low)	0.422 (0.234–0.761)	0.004	0.389 (0.218–0.695)	0.001

Abbreviations: TLS-tertiary lymphoid structures; OS-overall survival; DFS-disease-free survival; CEA-carcinoembryonic antigen; CA199-Carbohydrate antigen199

better prognosis in patients with a high TLS density. In addition, we determined whether a germinal center was present in the TLS using H&E staining (Figure 2C). Among the patients with the presence of TLS, the formation of a germinal center was observed in 32/108 (29.63%) patients, showing higher TLS density than those without a germinal center ( $p < 0.001$ ) (Figure 2D). Kaplan-Meier survival analysis revealed that TLS-high was significantly correlated with superior OS ( $p < 0.001$ ) and DFS ( $p < 0.001$ ) (Figures 2E,

2F). In gastric cancer with TLS, the presence of germinal center was still correlated with superior OS ( $p = 0.002$ ) and DFS ( $p = 0.004$ ) (Figures 2G, 2H). Cox regression univariate analysis indicated a significant association between TLS-high and longer OS and DFS (Supplementary Table S1). Among all the significant covariates in univariate analyses, TLS density and pTN stage were the only independent prognostic factors of both OS and DFS in multivariate Cox regression analysis (Table 2). Furthermore, a meta-analysis combining

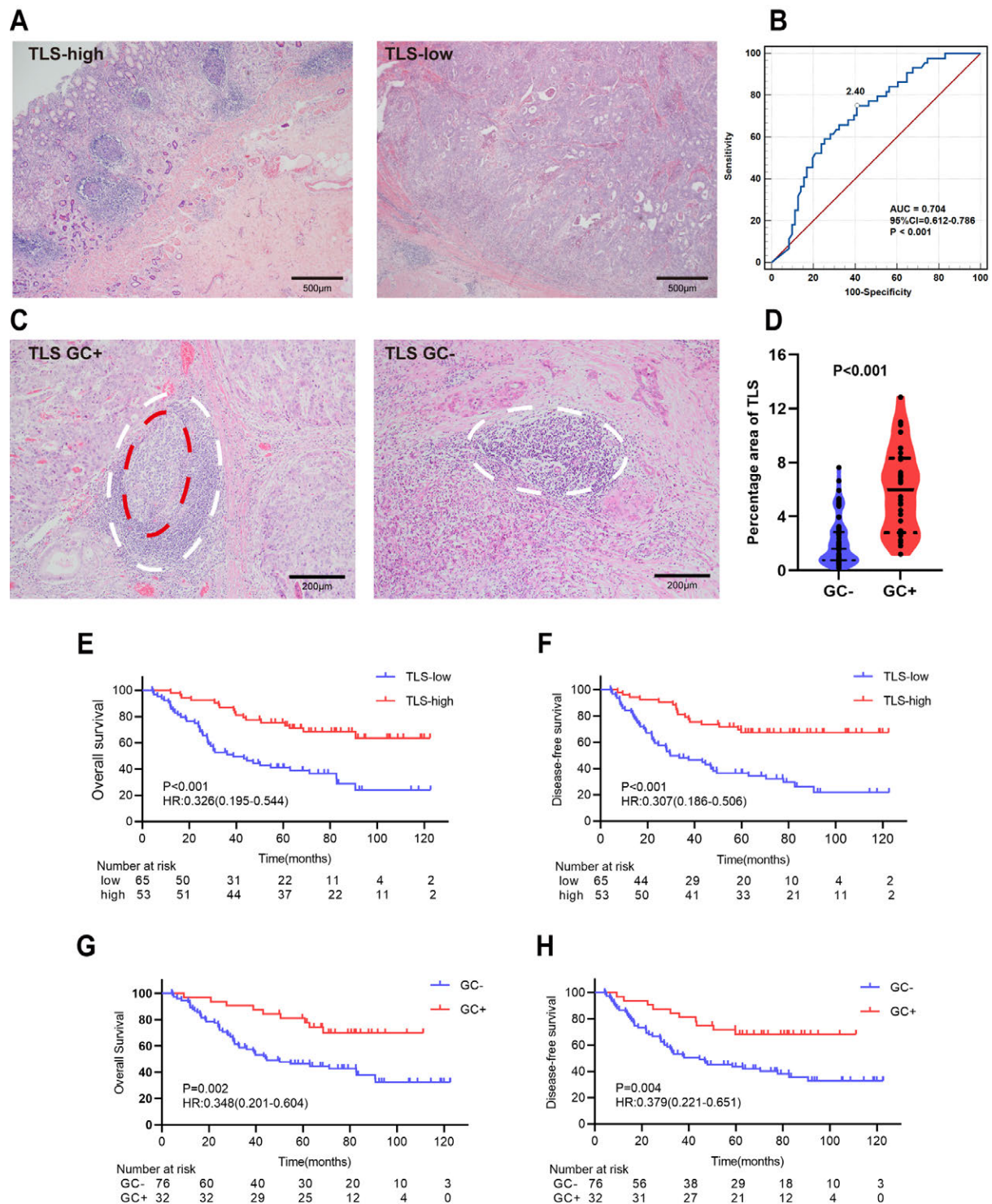


**Figure 2. Prognostic significance of TLS in gastric cancer patients.** A) Representative images of TLS identifying the TLS-high and TLS-low groups in H&E-stained sections. B) ROC identified 2.40 TLS density ratio as an optimal cut-off value for separating TLS-high and TLS-low tumors with prognostic correlation. C) Representative images of TLS with germinal center (GC+) and TLS without GC (GC-) in gastric cancer tissues by H&E staining and microscopic examination of a germinal center showed a pale area (red circle) with a dense outer region of lymphocytes (white circle). D) The density ratio of TLS was compared between gastric cancer patients positive or negative with the germinal center. E, F) Kaplan-Meier curves depicting OS and DFS for patients with high and low TLS density. G, H) Kaplan-Meier curves depicting OS and DFS for patients with positive GC and negative GC in TLS. Abbreviations: TLS-tertiary lymphoid structures; H&E-hematoxylin and eosin; ROC-receiver operating characteristic curve; AUC-area under curve; CI-confidence interval; HR-hazard ratio; GC-germinal center; OS-overall survival; DFS-disease-free survival.

TCGA and multiple GEO cohorts showed that gastric cancer patients with high TLS signature status also had a better prognosis (Figures 3A, 3B).

**Prognostic nomogram and validation of predictive accuracy.** Next, we attempted to construct a nomogram that incorporated TLS density and TNM stage to predict 3-year and 5-year survival probability among the patients with gastric cancer from the First Affiliated Hospital of Sun Yat-sen University. We also compared the predictive accuracy between the combined nomogram and the TNM stage. The combined nomogram for OS was established (Figure 4A). The nomogram c-index was superior to the c-index of the TNM stage alone (0.826 vs. 0.783,  $p < 0.001$ ). The calibration plots for 3-year and 5-year OS showed high consistency between the predicted and observed survival probabilities (Figures 4B, 4C). The combined nomogram for DFS is shown in Figure 4D. The nomogram c-index for DFS

was also superior to the c-index of the TNM stage (0.818 vs. 0.769,  $p < 0.001$ ). The calibration plots for 3-year and 5-year DFS also showed high consistency between the predicted and observed survival probabilities (Figures 4E, 4F).

**Tumor-infiltrating immune cells and TLS.** To determine whether TLS were associated with immune cell distribution in gastric cancer tissues, immunohistochemical staining was used to detect the infiltrating immune cells (Figure 5A). Considering the infiltration difference in the spatial distribution of immune cells in gastric cancer tissues, we divided immune cell infiltration into tumor center and invasive margin. The numbers of tumor-infiltrating CD3<sup>+</sup> T cells, CD8<sup>+</sup> T cells, and CD20<sup>+</sup> B cells were significantly greater in TLS-high tumor tissues than in TLS-low tumor tissues. In contrast, the number of CD68<sup>+</sup> TAMs in the TLS-high group was significantly lower than that in the TLS-low group. No significant differences in the levels of tumor-infiltrating

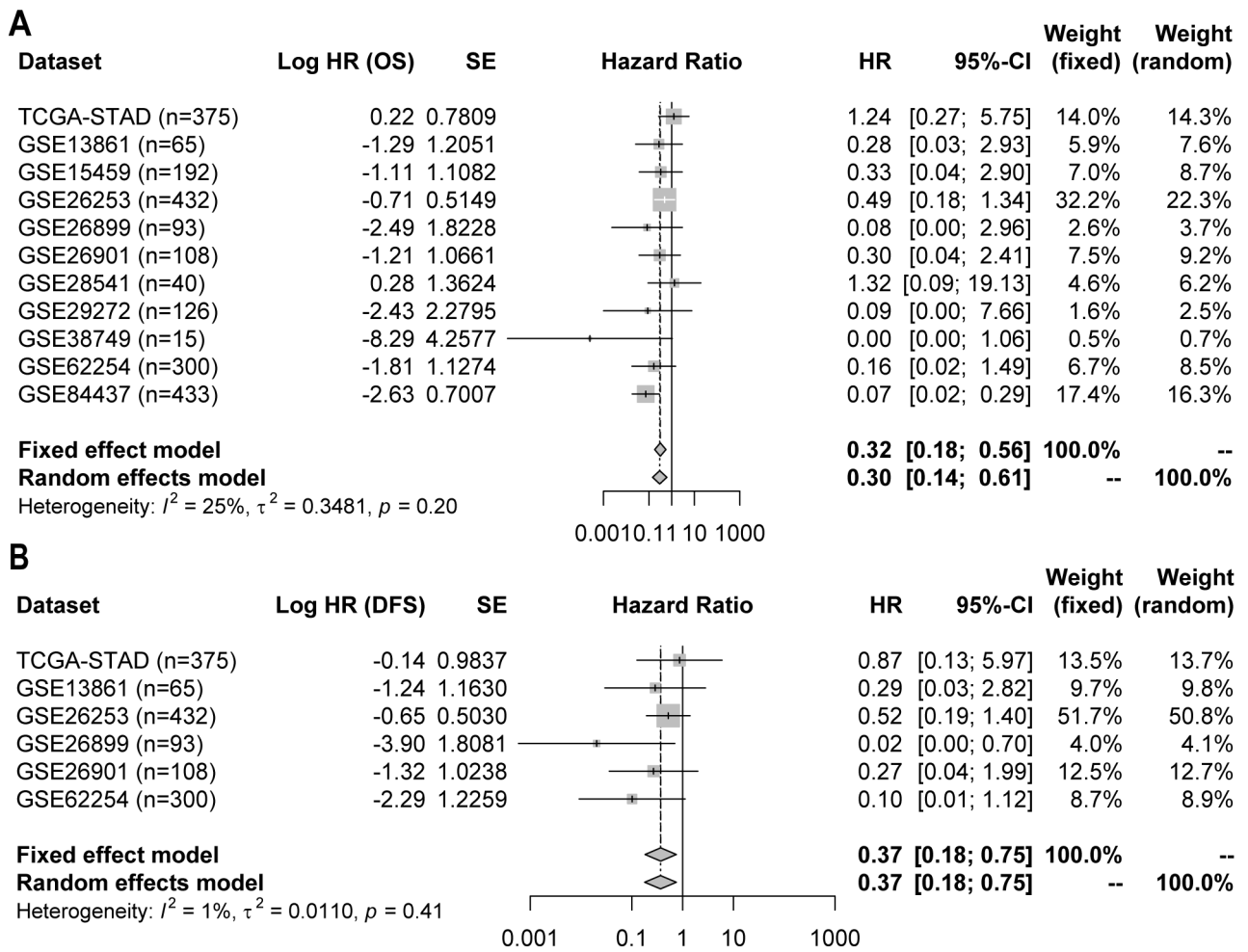


Figure 3. Forest plots for the association between TLS signature and survival among multiple gastric cancer cohorts. A) Overall survival (OS). B) Disease-free survival (DFS). Abbreviations: TLS-tertiary lymphoid structures; TCGA-STAD-the Cancer Genome Atlas Stomach Adenocarcinoma; GEO-Gene Expression Omnibus.

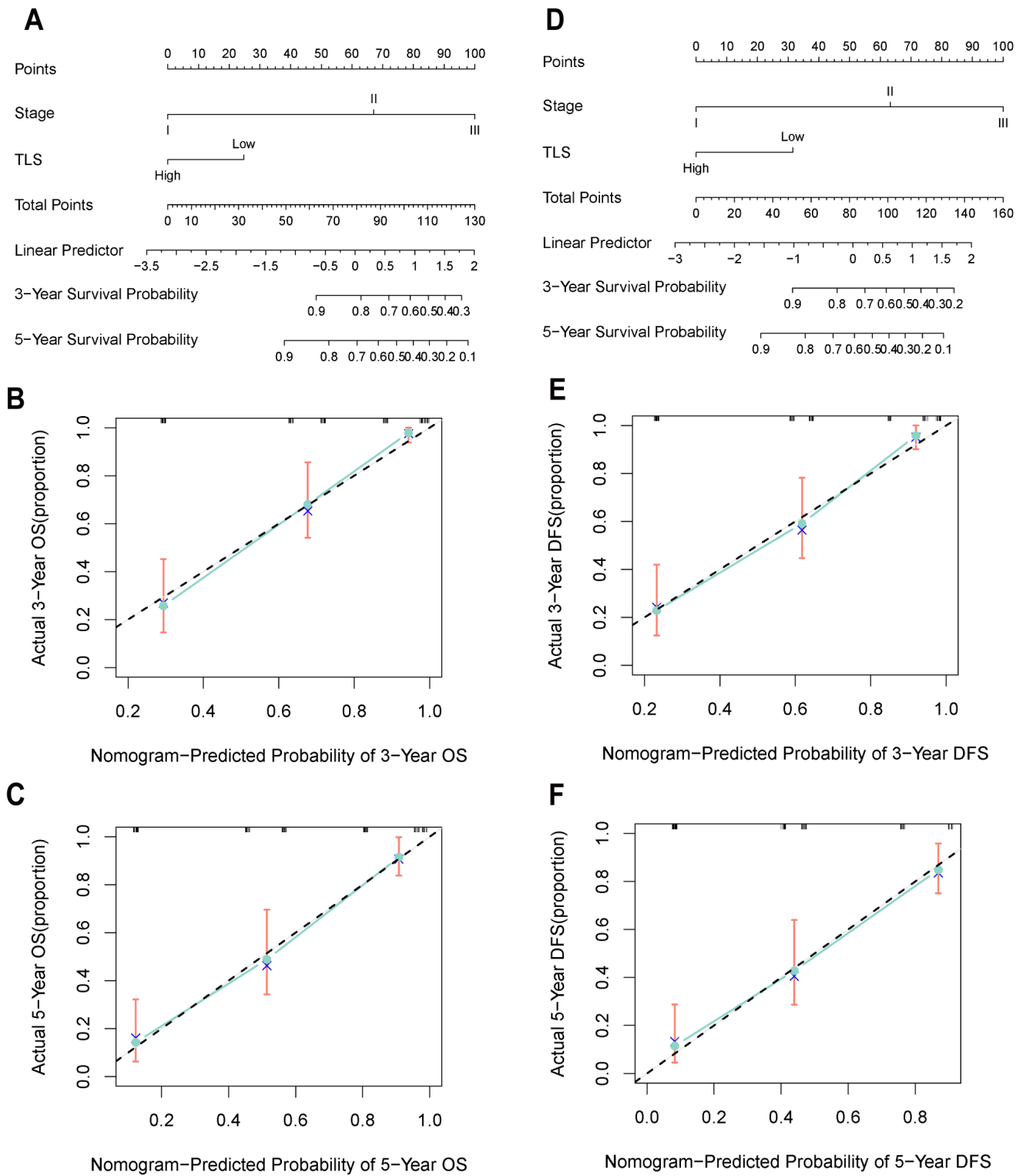


Figure 4. Nomogram for predicting prognosis and calibration plots in patients with gastric cancer. A) A predictive nomogram for 3-year and 5-year OS incorporating TLS density and TNM stage. B), C) Calibration plots of the nomogram for predicting the probability of 3-year (B), and 5-year (C) OS. D) A predictive nomogram for 3-year and 5-year DFS incorporating TLS density and TNM stage. E), F) Calibration plots of the nomogram for predicting the probability of 3-year (E), and 5-year (F) DFS. Abbreviations: TLS-tertiary lymphoid structures; TNM stage-tumor-node-metastasis stage; OS-overall survival; DFS-disease-free survival.

CD11c<sup>+</sup> DCs were observed based on the TLS density (Figure 5B). Moreover, xCell analysis also showed that high TLS signature status was significantly associated with more tumor-infiltrating immune cells, such as CD4<sup>+</sup> T cells, CD8<sup>+</sup> T cells, and B cells (Figure 5C). Additionally, GSEA analysis suggested that high TLS signature status was enriched in inflammation-related pathways and immune activation-related pathways (Figure 5D).

**TLS signature status and tumor molecular features.** To explore the potential mechanism that might influence TLS signature expression, we investigated the association of the TLS signature with pivotal molecular features in the TCGA-STAD cohort. Tumors with high TLS signature status showed a larger proportion of Epstein-Barr virus (EBV)-positive, microsatellite instability (MSI)-high, and hypermutated status, but a lower proportion of copy number variation

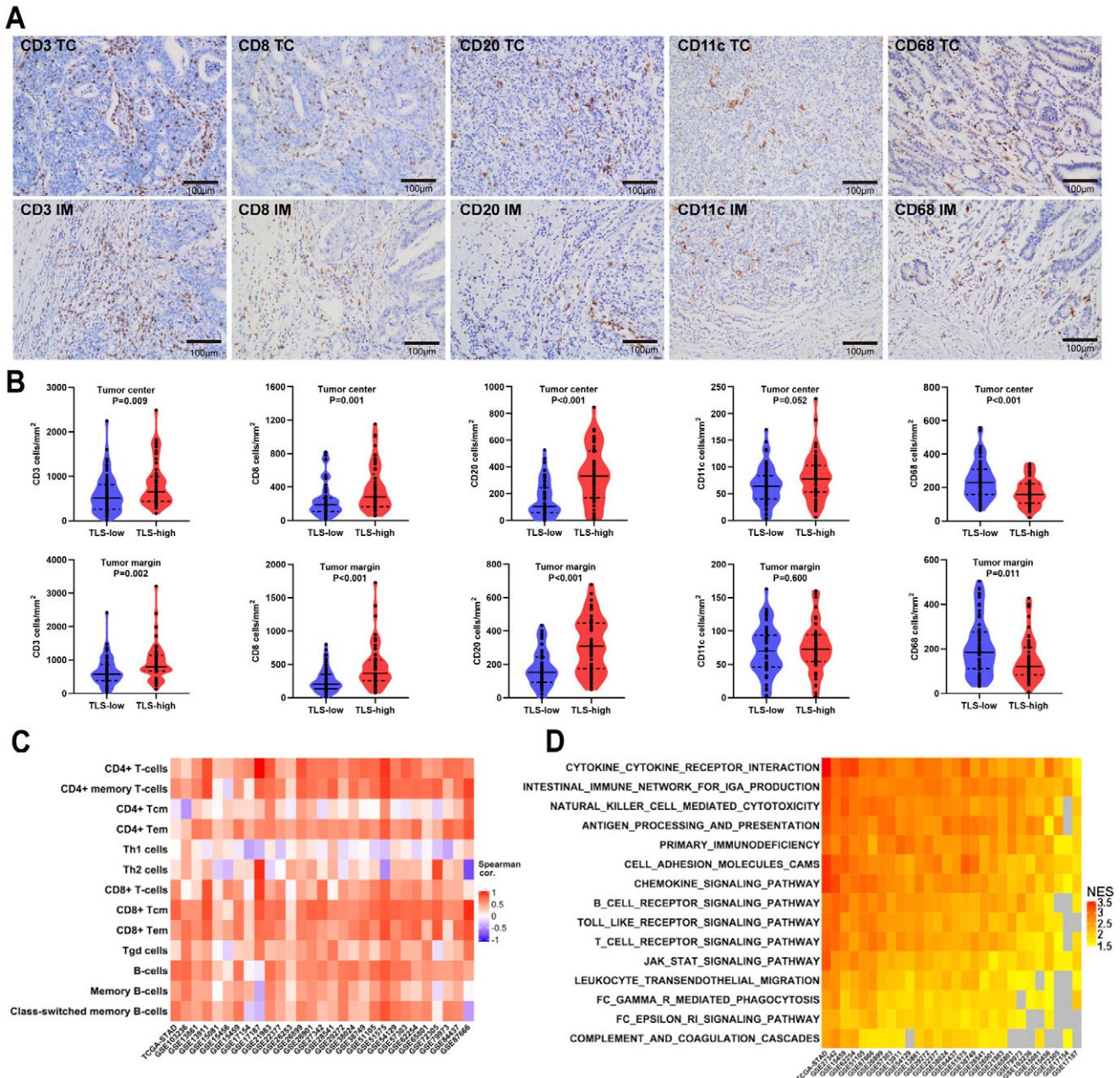


Figure 5. Association between TLS and tumor-infiltrating immune cells in gastric cancer. A) Representative images of tumor-infiltrated immune cells in the tumor center (TC) and invasive margin (IM). B) Statistical analyses of tumor-infiltrating immune cells with low or high TLS density. C) Heatmap showing the correlations between immune cell infiltration and TLS signature based on xCell estimation. D) Heatmap showing the NES in GSEA across TLS signature subtypes. Positive NES here means that the gene set is overrepresented at the top of a ranked list in the high TLS signature subtype compared with the low one. Abbreviations: TLS-tertiary lymphoid structures; NES-normalized enrichment score.

and whole-genome duplication (Table 3). The alterations of known oncogenic signaling pathways were further investigated, which suggested that patients with a low TLS signature status had a higher proportion of Erb-B2 receptor tyrosine kinase 2 (ERBB2) amplification and TP53 mutation, but less phosphoinositide 3-kinase (PI3K) mutation, compared with those with a high TLS signature (Figures 6A, 6B; Supplementary Figure S1A). Genes beyond known oncogenic signaling pathways were also investigated (Figure 6C), in which low-density lipoprotein receptor-related protein 1B (LRP1B) mutation was associated with low TLS signature level, whereas AT-rich interaction domain 1A (ARID1A) mutation was associated with high TLS signature level. We also found that a low TLS signature status was associated with a higher deletion frequency of members of the interferon (IFN) family (Supplementary Figure S1B). When analyzing the difference in DNA methylation profiles across the TLS subtypes, we found that EBV-positive status, accounting for a smaller proportion of patients, was a robust confounder in differential analysis (Supplementary Figure S1C). Thus, we also investigated the DNA methylation alterations across the TLS signature subtypes in EBV-negative patients only, which suggested that some immune-related transcript factors, such as growth factor-independent 1 transcriptional repressor (GFI1) and interferon regulatory factor4 (IRF4), were differentially epigenetically silenced in the TLS-low subgroup (Figure 6D).

## Discussion

We verified the hypothesis that the density of TLS was related to clinicopathological characteristics, patient prognosis, tumor-infiltrating immune cells, and key tumor molecular features. Overall, the results of the present study showed that high density and maturation of TLS were associated with longer OS and decreased risk of recurrence in gastric cancer. Furthermore, transcriptomics analysis based on multiple gastric cancer cohorts showed that a high TLS signature was strongly associated with inflammation-related pathways and immune activation-related pathways. In addition, our study showed that high TLS signature status was associated with key gastric cancer features, including EBV-positive status, MSI-high status, and hypermutated status.

The immune microenvironment has been extensively investigated over the past decade because of the remarkable advances in immunotherapy. TLS, a critical component of the tumor microenvironment, provides a local and essential microenvironment for both the innate and acquired immune systems to influence tumor progression, development, and metastasis [25]. Several studies have proposed the prognostic efficacy of TLS expression in various solid tumors [19, 26, 27]. Although the presence of TLS is largely associated with prolonged patient survival, several studies have detected TLS as a negative prognostic factor [28, 29]. These inconsistencies

**Table 3. Association between TLS signature status and tumor molecular features in the TCGA-STAD cohort.**

TCGA-STAD cohort	Level	TLS signature		
		TLS-low	TLS-high	p-value
All cases	375	188	187	
Molecular subtype (%)				<0.001
	EBV	4 (3.7)	19 (14.3)	
	MSI	13 (12.1)	34 (25.6)	
	CIN	73 (68.2)	49 (36.8)	
	GS	17 (15.9)	31 (23.3)	
Hypermutated status (%)				<0.001
	Yes	10 (9.5)	38 (28.8)	
	No	95 (90.5)	94 (71.2)	
Hypermethylation category (%)				<0.001
	Non-CIMP	109 (62.3)	95 (55.2)	
	CIMP-L	35 (20.0)	31 (18.0)	
	CIMP-H	28 (16.0)	22 (12.8)	
	CIMP EBV	3 (1.7)	24 (14.0)	
Copy number cluster (%)				<0.001
	High	76 (71.0)	58 (43.9)	
	Low	31 (29.0)	74 (56.1)	
Whole-genome duplication (%)				<0.001
	0	79 (45.7)	124 (73.4)	
	1	67 (38.7)	34 (20.1)	
	≥2	27 (15.6)	11 (6.5)	

Abbreviations: TLS-tertiary lymphoid structures; TCGA-STAD-The Cancer Genome Atlas Stomach Adenocarcinoma; EBV-Epstein-Barr virus; MSI-microsatellite instability; GS-genome stability; CIN-chromosomal instability; CIMP-CpG island methylator phenotype

in findings for different tumors might be explained by TLS location, heterogeneity of diagnostic methods for TLS, and their immune cell composition diversity [25]. Therefore, we used uniform criteria for the quantification of TLS, including TLS location and a normalization of the tumor area. We found that the high density of TLS was a good independent prognostic parameter for OS and DFS in gastric cancer. We constructed a nomogram model that combined the TNM stage and TLS status as prognostic variables and found that the nomogram predicted the prognosis of gastric cancer more accurately. In addition, the 19-gene signature has been proposed as a proxy for the presence of TLS in gastric cancer [8, 24]. To further strengthen our results, we used the TLS signature to evaluate the prognostic value of TLS in the TCGA-STAD cohort and multiple GEO cohorts. As we expected, patients harboring a high expression of TLS signature had better survival than patients with a low expression.

To gain a better understanding of the mechanism underlying the association between TLS and patient survival, we analyzed the infiltrating pattern of tumoral immune cells and the enrichment of tumor-related signaling pathways. We demonstrated that CD3<sup>+</sup> T cells, CD8<sup>+</sup> T cells, and CD20<sup>+</sup> B cells were more abundant in tumor tissues with a high density of TLS than in those with a low density of TLS. In

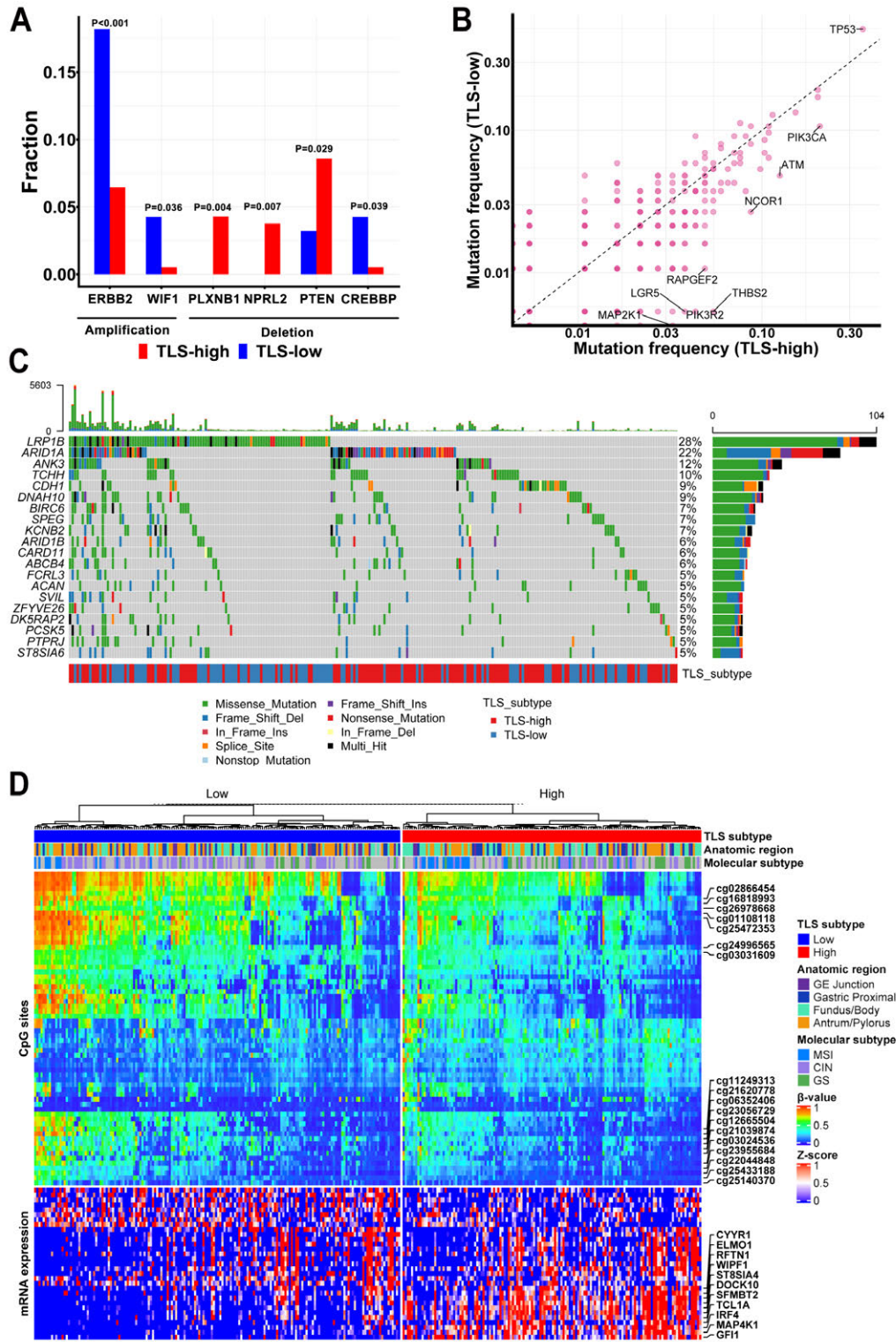


Figure 6. The landscape of molecular alterations between TLS-high signature and TLS-low signature in TCGA-STAD cohort. A) Significantly differential amplified or deleted genes in the oncogenic signaling pathways between the TLS-high/low subtypes. B) Correlation between TLS signature status and gene mutation frequency in the oncogenic signaling pathways. C) Waterfall plot depicting the correlations between somatic mutations beyond oncogenic signaling pathways and TLS signature status. D) Heatmap showing representative differentially epigenetically silenced genes and corresponding methylation profiles in promoter regions across TLS signature subtypes in EBV-negative gastric cancer. Abbreviations: TLS-tertiary lymphoid structures; TCGA-STAD-The Cancer Genome Atlas Stomach Adenocarcinoma; EBV-Epstein-Barr virus.

contrast, a higher density of CD68<sup>+</sup> TAMs in tumor tissues was significantly associated with a low density of TLS in gastric cancer patients. Our findings were similar to those of previous studies on hepatocellular carcinoma [30], lung cancer [31], and pancreatic cancer [32]. The beneficial impact of tumor-infiltrating T cells on clinical outcomes has been demonstrated in various cancers, and TLS could support the differentiation of CD8<sup>+</sup> T cells to enhance T cell-mediated anti-tumor responses [31, 33]. Tumor-infiltrating B cells are closely linked to the tumoral TLS and are considered to be actively involved in the immune response by directing T cell responses to antigens [34, 35]. CD68<sup>+</sup> TAMs, derived from the innate immune system, are associated with tumor progression and poor survival [36]. Furthermore, our findings showed that a high TLS signature was strongly associated with inflammation-related pathways and immune activation-related pathways. Given the close correlation between the high TLS density and immune-activating factors, TLS might render a more effective anti-tumor immune response and serve as a potential biomarker of effective immunotherapies.

The underlying mechanisms related to why TLS develop in some patients, but not in others, remain unknown. Because of the accumulation of genetic, epigenetic, and transcriptional alterations, tumors vary extensively in their molecular features [37]. Analysis of the tumor mutation background may explain the patient propensity of patients to form TLS within the tumor microenvironment. A recent study showed that a high TLS signature was associated with BRAF mutant, CpG island methylator phenotype-high (CIMP) status, and MSI-high status in colorectal cancer [38]. In addition, Lin et al. [26] reported that gastrointestinal stromal tumors with platelet-derived growth factor receptor  $\alpha$  mutations are more likely to be TLS-positive, which suggests an optimal prognosis. In our study, the tumors with high TLS signature exhibited higher EBV-positive status, MSI-high status, hypermutated status, and PI3K mutation. EBV-positive and MSI-high tumors have demonstrated intense T cell infiltrates and respond best to immune checkpoint inhibitors [39]. A recent study reported that activation of oncogenic pathways in tumor cells could influence a local antitumor immune response, and PI3K inhibitors could improve anti-PD1 efficacy [40, 41]. Therefore, key signaling molecules targeting TLS should be included in therapeutic strategies to induce an effective antitumor immune response.

In conclusion, this study demonstrated that high TLS density was associated with longer survival and recurrence time for gastric cancer patients who underwent surgical resection. Our study has revealed the strong association between TLS and the infiltration of immune cells into the tumors, suggesting that TLS may promote higher infiltration of effector immune cells. Furthermore, a high TLS signature status was associated with immune-activating pathway and key molecular features, indicating that TLS could represent the existence of continuous and effective anti-tumor immunity in the tumor microenvironment.

**Supplementary information** is available in the online version of the paper.

Acknowledgments: This work was supported by the National Natural Science Foundation of China (NO. 81772579).

## References

- [1] SUNG H, FERLAY J, SIEGEL RL, LAVERSANNE M, SOERJOMATARAM I et al. Global Cancer Statistics 2020: GLOBOCAN Estimates of Incidence and Mortality Worldwide for 36 Cancers in 185 Countries. *CA Cancer J Clin* 2021; 71: 209–249. <https://doi.org/10.3322/caac.21660>
- [2] SONGUN I, PUTTER H, KRANENBARG EM, SASAKO M, VAN DE VELDE CJ. Surgical treatment of gastric cancer: 15-year follow-up results of the randomised nationwide Dutch D1D2 trial. *Lancet Oncol* 2010; 11: 439–449. [https://doi.org/10.1016/s1470-2045\(10\)70070-x](https://doi.org/10.1016/s1470-2045(10)70070-x)
- [3] SMYTH EC, NILSSON M, GRABSCH HI, VAN GRIEKEN NC, LORDICK F. Gastric cancer. *Lancet* 2020; 396: 635–648. [https://doi.org/10.1016/s0140-6736\(20\)31288-5](https://doi.org/10.1016/s0140-6736(20)31288-5)
- [4] MAHONEY KM, RENNERT PD, FREEMAN GJ. Combination cancer immunotherapy and new immunomodulatory targets. *Nat Rev Drug Discov* 2015; 14: 561–584. <https://doi.org/10.1038/nrd4591>
- [5] XIN YJ, HODGE JB, OLIVA C, NEFTELINOV ST, HUBBARD-LUCEY VM et al. Trends in clinical development for PD-1/PD-L1 inhibitors. *Nat Rev Drug Discov* 2020; 19: 163–164. <https://doi.org/10.1038/d41573-019-00182-w>
- [6] JANJIGIAN YY, BENDELL J, CALVO E, KIM JW, ASCIERTO PA et al. CheckMate-032 Study: Efficacy and Safety of Nivolumab and Nivolumab Plus Ipilimumab in Patients With Metastatic Esophagogastric Cancer. *J Clin Oncol* 2018; 36: 2836–2844. <https://doi.org/10.1200/jco.2017.76.6212>
- [7] FUCHS CS, DOI T, JANG RW, MURO K, SATOH T et al. Safety and Efficacy of Pembrolizumab Monotherapy in Patients With Previously Treated Advanced Gastric and Gastroesophageal Junction Cancer: Phase 2 Clinical KEYNOTE-059 Trial. *JAMA Oncol* 2018; 4: e180013. <https://doi.org/10.1001/jamaoncol.2018.0013>
- [8] SAUTES-FRIDMAN C, PETITPREZ F, CALDERARO J, FRIDMAN WH. Tertiary lymphoid structures in the era of cancer immunotherapy. *Nat Rev Cancer* 2019; 19: 307–325. <https://doi.org/10.1038/s41568-019-0144-6>
- [9] POSCH F, SILINA K, LEIBL S, MÜNDLEIN A, MOCH H et al. Maturation of tertiary lymphoid structures and recurrence of stage II and III colorectal cancer. *Oncoimmunology* 2018; 7: e1378844. <https://doi.org/10.1080/2162402x.2017.1378844>
- [10] SILINA K, SOLTERMANN A, ATTAR FM, CASANOVA R, UCKELEY ZM et al. Germinal Centers Determine the Prognostic Relevance of Tertiary Lymphoid Structures and Are Impaired by Corticosteroids in Lung Squamous Cell Carcinoma. *Cancer Res* 2018; 78: 1308–1320. <https://doi.org/10.1158/0008-5472.Can-17-1987>

- [11] PIPI E, NAYAR S, GARDNER DH, COLAFRANCESCO S, SMITH C et al. Tertiary Lymphoid Structures: Autoimmunity Goes Local. *Front Immunol* 2018; 9: 1952. <https://doi.org/10.3389/fimmu.2018.01952>
- [12] GUNDERSON AJ, RAJAMANICKAM V, BUI C, BERNARD B, PUCILOWSKA J et al. Germinal center reactions in tertiary lymphoid structures associate with neoantigen burden, humoral immunity and long-term survivorship in pancreatic cancer. *Oncoimmunology* 2021; 10: 1900635. <https://doi.org/10.1080/2162402x.2021.1900635>
- [13] MUNOZ-ERAZO L, RHODES JL, MARION VC, KEMP RA. Tertiary lymphoid structures in cancer – considerations for patient prognosis. *Cell Mol Immunol* 2020; 17: 570–575. <https://doi.org/10.1038/s41423-020-0457-0>
- [14] LI H, LIU H, FU H, LI J, XU L et al. Peritumoral Tertiary Lymphoid Structures Correlate With Protective Immunity and Improved Prognosis in Patients With Hepatocellular Carcinoma. *Front Immunol* 2021; 12: 648812. <https://doi.org/10.3389/fimmu.2021.648812>
- [15] RAKAEE M, KILVAER TK, JAMALY S, BERG T, PAULSEN EE et al. Tertiary lymphoid structure score: a promising approach to refine the TNM staging in resected non-small cell lung cancer. *Br J Cancer* 2021; 124: 1680–1689. <https://doi.org/10.1038/s41416-021-01307-y>
- [16] SOFOPOULOS M, FORTIS SP, VAXEVANIS CK, SOTIRIADOU NN, ARNOGIANNAKI N et al. The prognostic significance of peritumoral tertiary lymphoid structures in breast cancer. *Cancer Immunol Immunother* 2019; 68: 1733–1745. <https://doi.org/10.1007/s00262-019-02407-8>
- [17] LYNCH KT, YOUNG SJ, MENEVEAU MO, WAGES NA, ENGELHARD VH et al. Heterogeneity in tertiary lymphoid structure B-cells correlates with patient survival in metastatic melanoma. *J Immunother Cancer* 2021; 9: e002273. <https://doi.org/10.1136/jitc-2020-002273>
- [18] HE W, ZHANG D, LIU H, CHEN T, XIE J et al. The High Level of Tertiary Lymphoid Structure Is Correlated With Superior Survival in Patients With Advanced Gastric Cancer. *Front Oncol* 2020; 10: 980. <https://doi.org/10.3389/fonc.2020.00980>
- [19] GERMAIN C, DEVI-MARULKAR P, KNOCKAERT S, BITON J, KAPLON H et al. Tertiary Lymphoid Structure-B Cells Narrow Regulatory T Cells Impact in Lung Cancer Patients. *Front Immunol* 2021; 12: 626776. <https://doi.org/10.3389/fimmu.2021.626776>
- [20] HELMINK BA, REDDY SM, GAO J, ZHANG S, BASAR R et al. B cells and tertiary lymphoid structures promote immunotherapy response. *Nature* 2020; 577: 549–555. <https://doi.org/10.1038/s41586-019-1922-8>
- [21] CALDERARO J, PETITPREZ F, BECHT E, LAURENT A, HIRSCH TZ et al. Intra-tumoral tertiary lymphoid structures are associated with a low risk of early recurrence of hepatocellular carcinoma. *J Hepatol* 2019; 70: 58–65. <https://doi.org/10.1016/j.jhep.2018.09.003>
- [22] OH SC, SOHN BH, CHEONG JH, KIM SB, LEE JE et al. Clinical and genomic landscape of gastric cancer with a mesenchymal phenotype. *Nat Commun* 2018; 9: 1777. <https://doi.org/10.1038/s41467-018-04179-8>
- [23] LIU Y, SETHI NS, HINOUE T, SCHNEIDER BG, CHERNICK AD et al. Comparative Molecular Analysis of Gastrointestinal Adenocarcinomas. *Cancer Cell* 2018; 33: 721–35.e8. <https://doi.org/10.1016/j.ccell.2018.03.010>
- [24] HENNEQUIN A, DERANGÈRE V, BOIDOT R, APETOH L, VINCENT J et al. Tumor infiltration by Tbet+ effector T cells and CD20+ B cells is associated with survival in gastric cancer patients. *Oncoimmunology* 2016; 5: e1054598. <https://doi.org/10.1080/2162402x.2015.1054598>
- [25] JACQUELOT N, TELLIER J, NUTT SL, BELZ GT. Tertiary lymphoid structures and B lymphocytes in cancer prognosis and response to immunotherapies. *Oncoimmunology* 2021; 10: 1900508. <https://doi.org/10.1080/2162402X.2021.1900508>
- [26] LIN Q, TAO P, WANG J, MA L, JIANG Q et al. Tumor-associated tertiary lymphoid structure predicts postoperative outcomes in patients with primary gastrointestinal stromal tumors. *Oncoimmunology* 2020; 9: 1747339. <https://doi.org/10.1080/2162402X.2020.1747339>
- [27] LI Q, LIU X, WANG D, WANG Y, LU H et al. Prognostic value of tertiary lymphoid structure and tumour infiltrating lymphocytes in oral squamous cell carcinoma. *Int J Oral Sci* 2020; 12: 24. <https://doi.org/10.1038/s41368-020-00092-3>
- [28] FINKIN S, YUAN D, STEIN I, TANIGUCHI K, WEBER A et al. Ectopic lymphoid structures function as microniches for tumor progenitor cells in hepatocellular carcinoma. *Nat Immunol* 2015; 16: 1235–1244. <https://doi.org/10.1038/ni.3290>
- [29] HILL DG, YU L, GAO H, BALIC JJ, WEST A et al. Hyperactive gp130/STAT3-driven gastric tumorigenesis promotes submucosal tertiary lymphoid structure development. *Int J Cancer* 2018; 143: 167–178. <https://doi.org/10.1002/ijc.31298>
- [30] LI H, WANG J, LIU H, LAN T, XU L et al. Existence of intratumoral tertiary lymphoid structures is associated with immune cells infiltration and predicts better prognosis in early-stage hepatocellular carcinoma. *Aging (Albany, NY)* 2020; 12: 3451–3472. <https://doi.org/10.18632/aging.102821>
- [31] DE CHAISEMARTIN L, GOC J, DAMOTTE D, VALIDIRE P, MAGDELEINAT P et al. Characterization of chemokines and adhesion molecules associated with T cell presence in tertiary lymphoid structures in human lung cancer. *Cancer Res* 2011; 71: 6391–6399. <https://doi.org/10.1158/0008-5472.Can-11-0952>
- [32] HIRAOKA N, INO Y, YAMAZAKI-ITOH R, KANAI Y, KOSUGE T et al. Intratumoral tertiary lymphoid organ is a favorable prognosticator in patients with pancreatic cancer. *Br J Cancer* 2015; 112: 1782–1790. <https://doi.org/10.1038/bjc.2015.145>
- [33] MARISA L, SVRCEK M, COLLURA A, BECHT E, CERVERA P et al. The Balance Between Cytotoxic T-cell Lymphocytes and Immune Checkpoint Expression in the Prognosis of Colon Tumors. *J Natl Cancer Inst* 2018; 110. <https://doi.org/10.1093/jnci/djx136>
- [34] LUND FE, RANDALL TD. Effector and regulatory B cells: modulators of CD4+ T cell immunity. *Nat Rev Immunol* 2010; 10: 236–247. <https://doi.org/10.1038/nri2729>

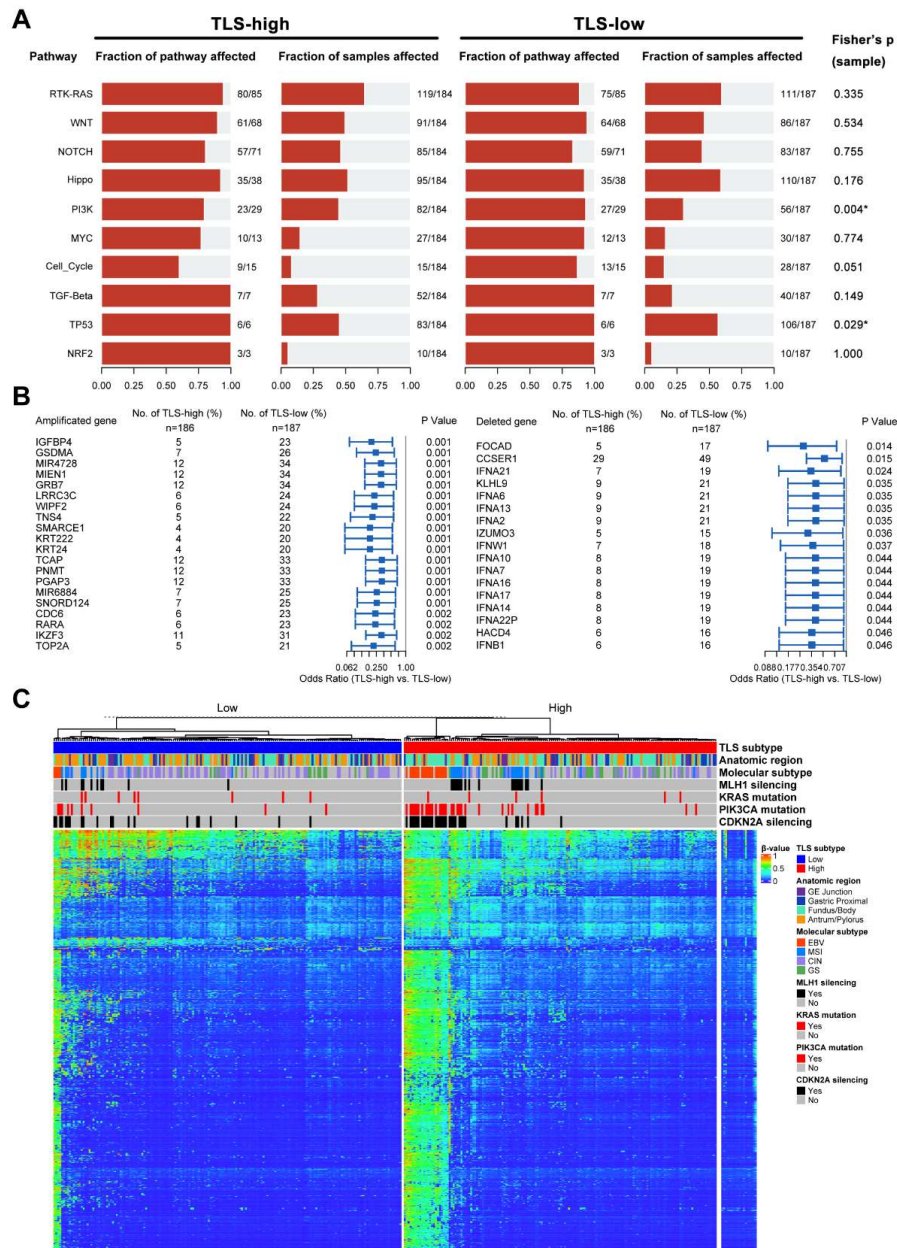
- [35] PETITPREZ F, DE REYNIÈS A, KEUNG EZ, CHEN TW, SUN CM et al. B cells are associated with survival and immunotherapy response in sarcoma. *Nature* 2020; 577: 556–560. <https://doi.org/10.1038/s41586-019-1906-8>
- [36] JEREMIASSEN M, BORG D, HEDNER C, SVENSSON M, NODIN B et al. Tumor-Associated CD68(+), CD163(+), and MARCO(+) Macrophages as Prognostic Biomarkers in Patients With Treatment-Naïve Gastroesophageal Adenocarcinoma. *Front Oncol* 2020; 10: 534761. <https://doi.org/10.3389/fonc.2020.534761>
- [37] HAUSSER J, ALON U. Tumour heterogeneity and the evolutionary trade-offs of cancer. *Nat Rev Cancer* 2020; 20: 247–257. <https://doi.org/10.1038/s41568-020-0241-6>
- [38] TOKUNAGA R, NAKAGAWA S, SAKAMOTO Y, NAKAMURA K, NASEEM M et al. 12-Chemokine signature, a predictor of tumor recurrence in colorectal cancer. *Int J Cancer* 2020; 147: 532–541. <https://doi.org/10.1002/ijc.32982>
- [39] KIM ST, CRISTESCU R, BASS AJ, KIM KM, ODEGAARD JI et al. Comprehensive molecular characterization of clinical responses to PD-1 inhibition in metastatic gastric cancer. *Nat Med* 2018; 24: 1449–1458. <https://doi.org/10.1038/s41591-018-0101-z>
- [40] SPRANGER S, GAJEWSKI TF. Impact of oncogenic pathways on evasion of antitumour immune responses. *Nat Rev Cancer* 2018; 18: 139–147. <https://doi.org/10.1038/nrc.2017.117>
- [41] SAI J, OWENS P, NOVITSKIY SV, HAWKINS OE, VILGELM AE et al. PI3K Inhibition Reduces Mammary Tumor Growth and Facilitates Antitumor Immunity and Anti-PD1 Responses. *Clin Cancer Res* 2017; 23: 3371–3384. <https://doi.org/10.1158/1078-0432.Ccr-16-2142>

[https://doi.org/10.4149/neo\\_2022\\_220128N123](https://doi.org/10.4149/neo_2022_220128N123)

# The association of immune cell infiltration and prognostic value of tertiary lymphoid structures in gastric cancer

Ji-Shang YU<sup>1,2,\*</sup>, Wei-Bin HUANG<sup>1,\*</sup>, Yu-Hui ZHANG<sup>1,\*</sup>, Jian CHEN<sup>1,2</sup>, Jin LI<sup>2,3</sup>, Hua-Feng FU<sup>1,2</sup>, Zhe-Wei WEI<sup>1,\*</sup>, Yu-Long HE<sup>1,3,\*</sup>

## Supplementary Information



Supplementary Figure S1. Relationships between TLS signature status and the mutation status or methylated modification. A) Oncogenic signaling pathways and their correlations with the TLS signature status in TCGA-STAD cohort. B) The top 20 amplified or deleted genes beyond oncogenic signaling pathways across the TLS signature subtypes. C) Heatmap showing DNA methylation features between TLS-high signature and TLS-low signature in the TCGA-STAD cohort. Abbreviations: TLS-tertiary lymphoid structures; TCGA-STAD-The Cancer Genome Atlas Stomach Adenocarcinoma; EBV-Epstein-Barr virus.

**Supplementary Table S1. Univariate analyses of OS and DFS with TLS and clinical characteristics in gastric cancer.**

Univariate analysis Variable	Overall survival		Disease-free survival	
	Hazard ratio (95%CI)	p-value	Hazard ratio (95%CI)	p-value
Gender (female/male)	0.678 (0.366–1.256)	0.217	1.347 (0.753–2.410)	0.316
Age (≥60years / <60years)	1.643 (0.984–2.742)	0.058	1.558 (0.946–2.566)	0.081
pT stage (T1+2/T3+T4)	9.514 (3.435–26.352)	<0.001	8.192 (3.268–20.535)	<0.001
pN stage (N0/N1+2+3)	8.119 (3.675–17.936)	<0.001	6.564 (3.225–13.361)	<0.001
Stage (III/I+II)	7.219 (3.958–13.168)	<0.001	6.282 (3.563–11.076)	<0.001
tumor location (antrum/no antrum)	1.611 (0.924–2.810)	0.093	1.598 (0.930–2.746)	0.09
tumor size (≥ 4cm/< 4cm)	2.865 (1.699–4.830)	<0.001	2.793 (1.683–4.634)	<0.001
Differentiation (undifferentiated/differentiated)	1.254 (0.747–2.106)	0.391	1.173 (0.709–1.940)	0.534
CEA (elevated/normal)	2.149 (1.258–3.671)	0.005	2.218 (1.315–3.741)	0.003
CA199 (elevated/normal)	3.564 (2.002–6.345)	<0.001	3.271 (1.846–5.794)	<0.001
Chemotherapy (yes/no)	0.652 (0.386–1.100)	0.109	0.583 (0.348–0.978)	0.041
TLS (high/low)	0.32 (0.181–0.564)	<0.001	0.302 (0.172–0.529)	<0.001

Abbreviations: TLS-tertiary lymphoid structures; OS-overall survival; DFS-disease-free survival; CEA-carcinoembryonic antigen; CA199-Carbohydrate antigen199